

Arabidopsis BRICK1/HSPC300 Is an Essential WAVE-Complex Subunit that Selectively Stabilizes the Arp2/3 Activator SCAR2

Jie Le,^{1,2} Eileen L. Mallery,^{1,2} Chunhua Zhang,¹ Steven Brankle,¹ and Daniel B. Szymanski^{1,*}

¹Department of Agronomy
Purdue University
Lilly Hall
915 W. State Street
West Lafayette, Indiana 47907

Summary

The actin cytoskeleton dynamically reorganizes the cytoplasm during cell morphogenesis. The actin-related protein (Arp)2/3 complex is a potent nucleator of actin filaments that controls a variety of endomembrane functions including the endocytic internalization of plasma membrane [1], vacuole biogenesis [2, 3], plasma-membrane protrusion in crawling cells [4], and membrane trafficking from the Golgi [5]. Therefore, Arp2/3 is an important signaling target during morphogenesis. The evolutionarily conserved Rac-WAVE-Arp2/3 pathway links actin filament nucleation to cell morphogenesis [6–9]. WAVE translates Rac-GTP signals into Arp2/3 activation by regulating the stability and/or localization of the activator subunit Scar/WAVE [8, 10–12]. The WAVE complex includes Sra1/PIR121/CYFIP1, Nap1/NAP125, Abi-1/Abi-2, Brick1(Brk1)/HSPC300, and Scar/WAVE [10, 13]: Defining the in vivo function of each subunit is an important step toward understanding this complicated signaling pathway. Brk1/HSPC300 has been the most recalcitrant WAVE-complex protein and has no known function. In this paper, we report that *Arabidopsis brick1* (*brk1*) is a member of the “distorted group” of trichome morphology mutants, a group that defines a WAVE-ARP2/3 morphogenesis pathway [14]. In this paper we provide the first strong genetic and biochemical evidence that BRK1 is a critical WAVE-complex subunit that selectively stabilizes the Arp2/3 activator SCAR2.

Results and Discussion

brk1 Is a “Distorted Group” Mutant and Functions within a WAVE-ARP2/3 Pathway

Arabidopsis trichomes are branched unicellular hairs that follow a highly reproducible morphogenetic program. Figures 1A and 1C are scanning electron microscopy (SEM) images of wild-type trichomes at several developmental stages. Microtubule-based branch initiation (stage 3) is followed by actin-dependent maintenance of polarized stalk and branch elongation (stage 4) [15, 16]. Following branch initiation, distorted mutants swell and twist in a highly variable manner. Although the distorted trichome phenotypes are the most striking,

epidermal shape and adhesion are affected throughout the shoot. Each of the eight known distorted mutants corresponds to a WAVE- or ARP2/3-complex subunit-encoding gene [14]. In this paper, WAVE and ARP2/3 refer to the entire complex or the collective functions of the subunit-encoding genes. Double-mutant analyses and biochemical data indicate that *Arabidopsis* WAVE positively regulates ARP2/3 [9, 17]. WAVE-dependent positive regulation of ARP2/3 involves the Scar homolog SCAR2/DIS3/ITB3 [9, 18]. Scar/WAVE proteins potently enhance the nucleation activity of Arp2/3 [19, 20]. Regulation of Scar activity appears to be the primary function of the WAVE complex; however, the control mechanism is unclear [21]. Assembly of Scar into a WAVE complex may negatively regulate its ability to activate Arp2/3 [8, 10], prevent Scar degradation [8, 11], or regulate Scar localization in response to activating signals [12].

On the basis of the high level of amino acid identity between *Arabidopsis* BRK1 and other HSPC300 homologs (Figure 2A) and of its potential allelism with the genetically linked but unknown distorted mutant *doughboy* (D.S., unpublished data), we tested for *BRK1* function in the WAVE-ARP2/3 pathway. The *brk1-1* and *brk1-2* nonsense mutants were generated by using the reverse-genetic approach termed TILLING [22]. Each of the three independently generated *brk1* alleles caused strong and stage-specific trichome swelling, twisting, and a reduced branch length that is characteristic of the distorted group (Figures 1B and 1D), but none of them were allelic to *doughboy*. Like other “distorted group” mutations, *brk1-1* and *brk1-2* segregate as monogenic recessive alleles on the basis of both the wild-type phenotype of F1 backcross individuals ($n = 34$) and the 3:1 segregation of wild-type:mutant plants in F2 populations ($\chi^2 = 0.8$, $p > 0.3$). We confirmed the TILLING-facility *brk1* allele sequencing data with PCR-based molecular markers (Figure 2B). In segregating populations, the *brk1-1* ($n = 26$ chromosomes) and *brk1-2* ($n = 32$ chromosomes) phenotypes cosegregate perfectly with the associated nonsense mutations. In addition, crosses between *brk1-1* and *brk1-2* plants failed to complement mutant phenotypes. Therefore, two independent *brk1-1* alleles (each causing an identical mutation) and the unique *brk1-2* allele disrupt the coding of the BRK1 gene and cause trichome distortion. The finding that three independent *brk1* alleles cause identical trichome distortion phenotypes is proof that the cell-shape defects are caused by *BRK1* gene disruption. The *brk1-1* and *brk1-2* alleles probably reflect the null phenotype, because both alleles severely truncate the wild-type protein and cause an identical array of phenotypes with indistinguishable severity.

We next tested for involvement of *BRK1* in a WAVE-ARP2/3 actin filament nucleation pathway. In cultured *Drosophila* S2 cells, *HSPC300* appears to be resistant to RNA interference (RNAi), and on the basis of the mild knockdown phenotype of *hspc300* relative to other *wave* and *arp2/3* RNAi lines, the gene does not clearly

*Correspondence: dszyman@purdue.edu

²These authors contributed equally to this manuscript.

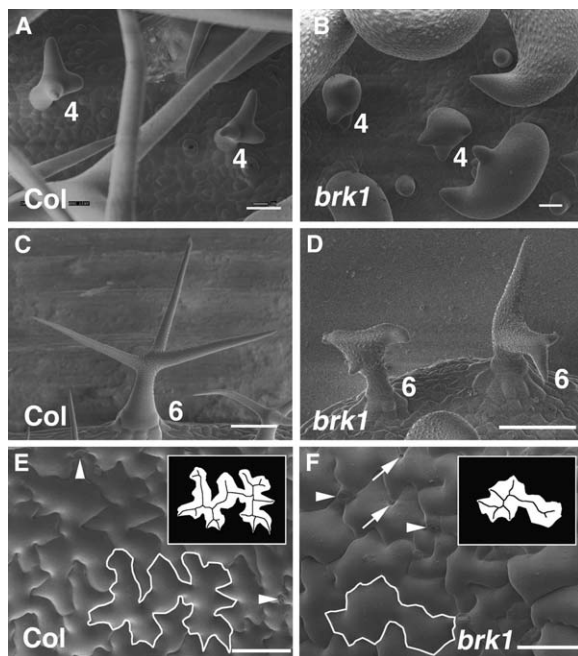


Figure 1. The *BRK1* Mutation Causes an Array of Phenotypes that Defines the “Distorted Group” of Morphology Mutants

(A and B) SEM images of stage 4 trichomes on upper surface of developing wild-type and *brk1* leaves.

(C and D) SEM images of stage 6 trichomes of wild-type and *brk1*.

(E and F) SEM micrographs of upper surface of 12 DAG cotyledons taken from wild-type and *brk1* plants. Insets are calculated skeletons that overlay the thresholded image of the highlighted pavement cells in same panel. Numbers at the lower right side of a trichome indicate the developmental stages. White arrows indicate the gaps between adjacent pavement cells; arrowheads indicate the stomatal pores. Scale bars represent 20 μ m.

fall within the pathway [11]. Mutation of maize *Brick1* causes numerous epidermal cell-shape defects [23], but *WAVE* and *Arp2/3* gene functions have not been defined in this system. If *Arabidopsis BRK1*, *WAVE*, and *ARP2/3* define a common pathway, all of the genes should have an overlapping expression pattern. Like other *WAVE* and *ARP2/3* subunit-encoding genes [9], *BRK1* also accumulates in several major organ types (Figure 2C). Microarray experiments that exhaustively analyzed gene expression throughout plant development also detect an overlapping expression pattern for *BRK1*, *WAVE*, and *ARP2/3* genes [24].

Strong evidence that *BRK1* functions within a *WAVE-ARP2/3* pathway comes from the comparison of *brk1* phenotypes to those of known *wave* and *arp2/3* strains. If *BRK1* functions in the pathway, the mutant should have an identical array of phenotypes. The extent of swelling in *brk1* stage 4 trichomes (Figure 1B) is similar to that in *wave* and *arp2/3* hairs. Forty-five percent ($n = 11$) of *brk1* stage 4 trichomes have a maximum diameter greater than 30 μ m, and all mature trichomes have a reduced trichome branch length compared with the wild-type (Figure 1D, Table 1). Etiolated *brk1* seedlings, like all known *wave* and *arp2/3* plants, have a significantly reduced mean hypocotyl length compared with the wild-type (Table 1). *Brk1*⁻ plants also have numerous gaps between pavement cells (Figure 1F) and within files

of hypocotyl epidermal cells (Figure S1 in the Supplemental Data available online). No such cell-cell adhesion defects are seen in the wild-type (Figure 1E, Figure S1).

We also examined the organization of the actin cytoskeleton in whole-mounted *brk1* trichomes at the onset of the mutant phenotype during stage 4. In addition to a dense meshwork of cortical actin filaments, wild-type trichomes at this stage generate in the core cytoplasm a population of actin bundles that are aligned with the long axis of the branch. The actin cables extend to the cell cortex along the apical dome of the developing branch (Figure 3A). Similarly staged *wave* and *arp2/3* branches have an extensive actin cytoskeleton, but there are fewer bundles, and they lack a similar polarized alignment [17, 25–29]. Developing *brk1* trichomes also fall into this category. Elongating *brk1* branches contain fewer actin bundles, and/or the cables fail to extend fully toward the branch apex (Figure 3B). Compared with 100% ($n = 6$) of wild-type stage 4 branches that contain properly aligned bundles, only 31% ($n = 13$) of similarly staged *brk1* branches have such an arrangement. This percentage for *brk1* branches is similar to what has been reported for *arp2/3* mutants, but is more severe than known *nap1* and *sra1* actin defects [28, 29]. Mature wild-type trichomes contain primarily cortical actin bundles that are loosely aligned with the main axis of the stalk and branches (Figure 3C). Elongated regions of *brk1* branches have a similar arrangement of actin bundles, but locations of severely disorganized actin filaments correlate with regions of cell swelling (Figure 3D). Despite the presence of actin-based defects in distorted mutants, the identity and functions of ARP2/3-generated actin filaments in plant cells are not known. Nonetheless, the findings that *brk1*, *wave*, and *arp2/3* have distorted trichomes, similar actin defects, indistinguishable cell-cell adhesion defects, and a reduced hypocotyl length provide strong evidence that these genes function in a common pathway.

Maize *brk1* leaf epidermal cells completely lack the crenulation that occurs along the lateral cell borders. *Arabidopsis brk1* pavement cells, like those of known *WAVE* and *ARP2/3* mutants [25, 27, 29], are clearly capable of lobe formation (Figure 1F). However, *wave* and *arp2/3* pavement-cell phenotypes ranging from small cells with a near absence of lobes [3] to subtle quantitative reductions in cell-shape complexity [30–32] have been reported. Circularity is a quantitative descriptor of shape complexity [33] and is a useful assay for pavement-cell shape [31, 34]. A circle has a circularity of 1, and as the perimeter increases relative to area, the value decreases. For each genotype, we outlined individual pavement cells from digital SEM or fluorescence images and measured their perimeter and area (see Supplemental Experimental Procedures). The mean circularity of 0.43 for *brk1* pavement cells was significantly greater than the mean value of 0.23 for wild-type. For comparison, maize *brk1* and wild-type cells have circularity values of approximately 0.5 and 0.1, respectively (D.S. and J.L., unpublished data).

In order to gain more information about the geometric basis of the *brk1* circularity phenotype, we developed an objective procedure to count pavement-cell lobes. Because lobes are lateral protrusions from the cell boundary, the feature can be recognized by a medial-axis

Table 1. Comparison of *brk1* Phenotypes to those of Col, *arpc2*, *sra1*, and *scar2* Plants

	<i>brk1-1 (hspc300)</i>	Col-0 (Wild Type)	<i>arpc2 (dis2-1)</i>	<i>sra1 (pir)</i>	<i>scar2 (dis3)</i>
Trichome Branch Length (μm)					
Branch 1	73 \pm 28 ^a (n = 10)	297 \pm 43** (n = 9)	74 \pm 49 (n = 7)	176 \pm 89* (n = 7)	198 \pm 58** (n = 9)
Branch 2	35 \pm 12 (n = 10)	243 \pm 64** (n = 9)	23 \pm 12 (n = 7)	77 \pm 49 (n = 7)	132 \pm 42** (n = 9)
Branch 3	17 \pm 11 (n = 10)	188 \pm 34** (n = 9)	17 \pm 5 (n = 7)	40 \pm 33 (n = 7)	98 \pm 37** (n = 9)
Etiolated Hypocotyls Total Length (mm)					
	10.6 \pm 2.0 (n = 10)	18.5 \pm 1.8** (n = 10)	11.9 \pm 2.0 (n = 10)	12.5 \pm 1.8 (n = 10)	N. D.
Pavement-Cell Size ($\times 10^4 \mu\text{m}^2$)					
	1.29 \pm 0.35 (n = 29)	1.98 \pm 0.62** (n = 25)	1.74 \pm 0.37* (n = 24)	1.65 \pm 0.34* (n = 26)	1.62 \pm 0.31* (n = 23)
Pavement-Cell Shape					
Circularity ^b	0.43 \pm 0.09 (n = 29)	0.22 \pm 0.05** (n = 25)	0.39 \pm 0.07 (n = 24)	0.35 \pm 0.04** (n = 26)	0.26 \pm 0.05** (n = 23)
Skeleton ends ^c	5.6 \pm 2.1 (n = 29)	11.4 \pm 2.8** (n = 25)	6.9 \pm 1.9 (n = 24)	6.0 \pm 2.0 (n = 26)	10.2 \pm 2.4** (n = 23)

* and ** indicate significant difference from *brk1* according to a Student's t test for trichome branches and an ANOVA Bonferroni multiple-comparison test for hypocotyls and pavement cells. *p value < 0.05; **p value < 0.001.

^a Mean value \pm standard deviation.

^b Circularity is a descriptor of shape complexity.

^c Number of skeleton end points calculated from the medial-axis transformation of thresholded individual pavement-cell images.

to an effect of the *er-105* that was used in the TILLING project, because for all of the phenotypes shown in Table 1, Col-0 *er-105* plants were indistinguishable from Col-0 (data not shown). The phenotype is not due to background mutations because large numbers of small cotyledon pavement cells have been seen in *brk1* plants sampled from several segregating backcross populations. *Brk1*⁻ cotyledons compensate for a decreased mean size by increasing cell number because the mean cotyledon area of *Brk1*⁻ plants does not differ from the wild-type, *sra1*, and *arpc2* (data not shown). Cell size control may be a *WAVE-ARP2/3*-independent function for BRK1. The finding that a significant fraction

of HSPC300 is free and soluble [39] is consistent with protein functions that are independent of the fully assembled WAVE complex. However, because BRK1 physically interacts with multiple SCAR isoforms [40], and potentially with additional WAVE-complex proteins [39], hypothesized novel BRK1 pathways may involve a subset of WAVE-complex proteins.

BRK1 is a Critical WAVE Subunit that Selectively Stabilizes SCAR2

In order to evaluate the relative importance of BRK1 in the *WAVE-ARP2/3* pathway, we compared the severity of *brk1* phenotypes with those of strains that are null

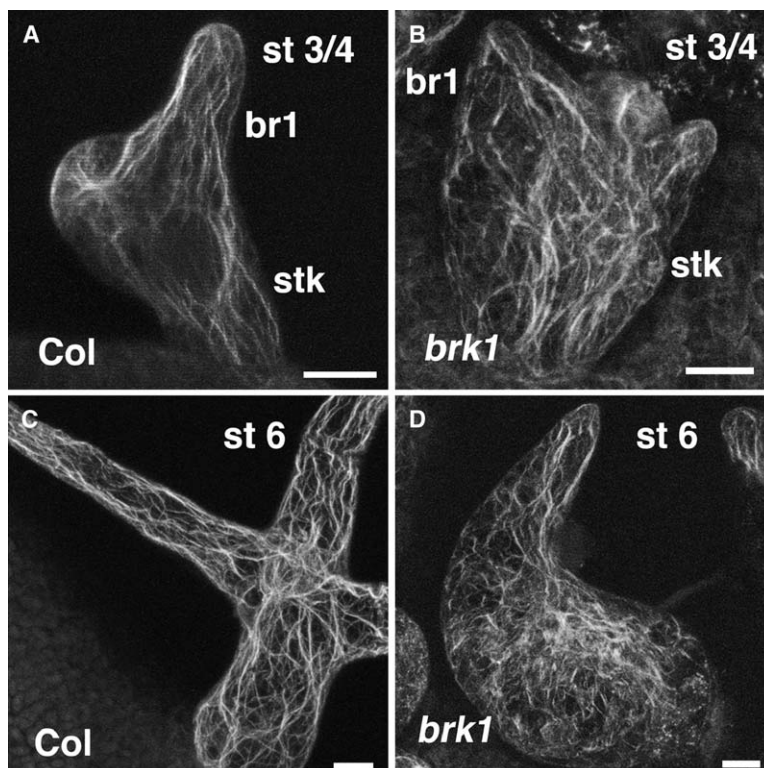


Figure 3. Actin Bundles Are Disorganized in *brk1* Trichomes at Early and Late Developmental Stages

(A and B) Actin organization in wild-type and *brk1* stage 3/4 trichomes.

(C and D) Actin organization in wild-type and *brk1* stage 6 trichomes.

Actin bundles in trichomes are visualized by using fluorescent phalloidin as previously described [26]. Images in the panels are projections of the whole cell. st 3/4 denotes stage 3/4, a cell with both emerging and elongating branch buds with a blunt tip; st 6 denotes stage 6, a mature trichome with papillae on the cell wall surface; br1 denotes branch 1; and stk denotes stalk. The scale bar represents 10 μm .

for other *WAVE*- and *ARP2/3*-subunit genes. A comparison of trichome branch length is the most sensitive assay to resolve differences between *wave* and *arp2/3* mutants. First, it is clear from our morphometric analyses that *brk1* trichome and pavement-cell phenotypes are more severe than those of *scar2*. This is expected because *SCAR2* functions redundantly with other *SCAR* paralogs, and *scar2* phenotypes are the weakest among the known distorted mutants [9, 18]. As stated above, the extent of *brk1* actin cytoskeleton disorganization is greater than what has been published for *nap1* and *pir* mutants. In addition, the mean trichome length of *brk1* is significantly less than *sra1*. However, *brk1* trichome branch defects are not more severe than *arpc2* (Table 1). The similar trichome phenotype of *Brk1*⁻ and *Arpc2*⁻ indicates that *Brk1*⁻ reflects the *WAVE* null phenotype, and it argues against hypothesized *WAVE*-independent *ARP2/3* activation pathways [14]. *WAVE* may be the primary pathway for *ARP2/3* activation throughout the plant, because in pairwise statistical tests, *Brk1*⁻ pavement-cell shape complexity was significantly reduced compared with *Sra1*⁻, but was indistinguishable from *Arpc2*⁻ (Table 1). Our assays for hypocotyl length and pavement-cell lobe number did not clearly distinguish *brk1*, *arpc2*, and *sra1*. Compared to circularity values, the medial-axis transformation procedure may not be as sensitive to small or symmetrical undulations in the cell perimeter.

The severe *brk1* phenotypes are surprising. HSPC300 is a peripheral *WAVE*-complex protein that affects neither complex assembly [39] nor the ability of the complex to activate *Arp2/3* in vitro [13]. One function of *WAVE*-complex proteins is to protect the *Scar/WAVE* subunit from proteasome-dependent degradation [8, 11]. Among the four *Arabidopsis* *Scar* paralogs, only *SCAR2* is known to function within the *WAVE-ARP2/3* pathway [9, 18]. Therefore, we assayed *SCAR2* protein levels in whole-shoot protein extracts isolated from wild-type, *sra1*, *nap1*, *scar2*, and *brk1* plants. The *SCAR2* antibody is specific, because the *SCAR2* band was not detected in *scar2* extracts (Figure 4A, lane 4). In three independent experiments, *SCAR2* accumulates to similar levels in Col, *sra1*, and *nap1* backgrounds (Figure 4, lanes 1–3) and is also present in *arpc2* extracts (data not shown). Because *sra1* plants have clear phenotypes, the *SCAR2* protein in the mutant is not completely functional. Human and plant *SRA1* homologs are direct *Rac1/ROP* effectors [29, 41] that may couple small GTPase activation signals to regulated localization of the *WAVE* complex [12]. Therefore, *sra1* phenotypes may be due to the failure to translate *AtROP* signals into a fully functional *SCAR2* response. Alternatively, there may be additional *SRA1*-independent *WAVE* activation pathways that lead to partial *SCAR2* function.

The *brk1* phenotype is associated with a severe decrease in *SCAR2* protein accumulation, a decrease that is unique to *brk1* (Figure 4, lane 5). In three independent trials, the mean level of *SCAR2* is reduced more than 60-fold in *brk1* compared with the wild-type. It is possible that the strong *brk1* phenotype is caused by the degradation of all *WAVE*-complex proteins. For example, in *Drosophila*, *SRA1* (*CYFIP*), *NAP1* (*Kette*), and *Scar* protein stability have a high degree of interdependence [42]. We therefore tested for the presence of

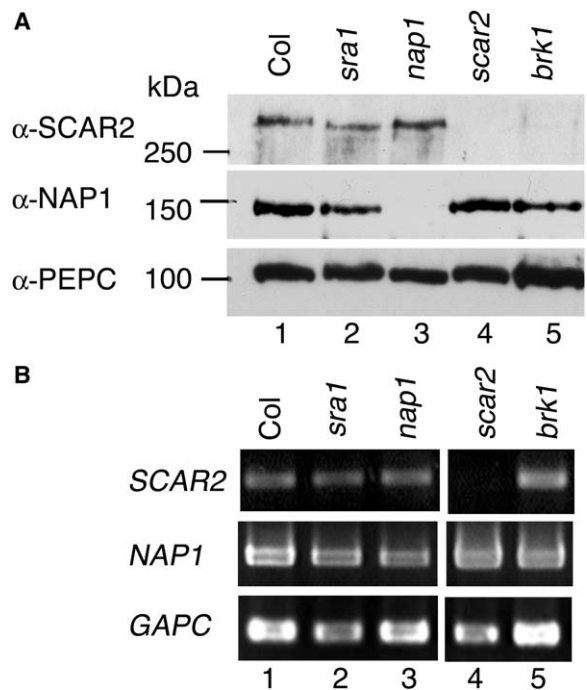


Figure 4. Loss of BRK1 Selectively Destabilizes the Arp2/3 Activator SCAR2

(A) Western-blot analysis of SCAR2 (upper panel), NAP1 (middle panel), and PEPC (lower panel, loading control) in protein extracts from several *wave* mutants that are labeled at the top of the panel. The position of the protein standards is shown on the left side of the blot.

(B) RT-PCR analysis indicating transcript levels of *SCAR2*, *NAP1*, and *GAPC* in the same backgrounds used in panel (A). The *dis3-1* (*scar2*) allele causes premature transcriptional termination of *SCAR2* [9], and therefore the transcript is not detected. The *GAPC* control proves that the RNA samples are intact. The primer sequences for *SCAR2* are described in [9]. The *NAP1GRL* transcript from exons 10 to 19 was tested with the same primers as in [28].

NAP1 in the same *wave* backgrounds described above. The *NAP1* antibody recognizes a specific protein that is of the predicted size and is not present in *nap1* extracts (Figure 4A, lanes 1 and 3). In triplicate experiments, *NAP1* levels in *sra1*, *scar2*, and *brk1* shoot extracts did not differ significantly from the wild-type. These data indicate that the *BRK1*-dependent stabilization of *SCAR2* is selective, and that the mutation does not cause global *WAVE*-subunit degradation. We ruled out the possibility that the absence of *SCAR2* in *brk1* could be explained by a failure to accumulate *SCAR2* RNA. Total RNA was isolated from the same set of *WAVE* mutants, and the *SCAR2* transcript was detected by using reverse transcription (RT)-PCR. *SCAR2* transcripts are detected at similar levels in wild-type and *brk1* plants (Figure 4B, lanes 1 and 5). Therefore, the most likely explanation is that *BRK1* selectively stabilizes *SCAR2*. If *SCAR2* stability is *BRK1*-dependent, *brk1* single-mutant and *brk1 scar2* double-mutant phenotypes should be identical. We isolated several *brk1 scar2* mutants from a segregating F2 population. As expected, the trichome branch length and cotyledon pavement-cell circularity and area of *brk1 scar2* are indistinguishable from those of *brk1* siblings. Therefore, the genes function in a common

pathway, and residual SCAR2 activity is not apparent in *brk1* mutants.

We favor a model in which BRK1 binds to SCAR2 and increases its stability. It has been shown that BRK1/HSPC300 physically interacts with Scar/WAVE proteins [13, 39], and that the interaction occurs through the conserved N-terminal Scar homology domain (SHD) [40]. *Arabidopsis* BRK1 physically interacts with the same domain of SCAR2 [18]. Because *Arabidopsis* has retained all of the WAVE-complex protein domains that are required for complex assembly, we expect the plant data to be of predictive value for other multicellular organisms that utilize BRK1/HSPC300-SHD binding interactions. In cultured *Drosophila* cells, the level of Scar protein in *wave* backgrounds can be increased by poisoning the proteasome with an inhibitor [11]. *Arabidopsis* BRK1 may bind SCAR2 and mask a determinant of proteasome-dependent degradation. If this model is correct, BRK1 may stabilize SCAR2 in free or complex-bound forms as it is synthesized or as it is recycled during multiple rounds of ARP2/3 activation, release, and sequestration.

Clearly, destabilization of SCAR2 alone does not explain the severe *brk1* phenotype, because *scar2* phenotypes are much less severe than those of *brk1*. SCAR2 is likely to function redundantly with SCAR1, SCAR3, and/or SCAR4, each of which encodes both an SHD and a predicted C-terminal Arp2/3 activation domain termed WA [9, 18]. Because BRK1 is likely to bind to the SHD of all *Arabidopsis* SCARs, we propose that the entire SCAR gene family is functionally eliminated by the loss of BRK1. In this scenario, *brk1* phenotypes resemble those of *arp2/3* plants because the WAVE activation pathway has been completely eliminated. However, compared with SCAR2, SCAR3 and SCAR4 appear to activate bovine Arp2/3 with greatly reduced efficiency [9, 40]. Therefore the SCAR paralogs that function in the WAVE-Arp2/3 pathway remain to be identified. A better understanding of BRK1-SCAR morphogenesis pathways requires additional genetic and biochemical analyses.

Supplemental Data

Supplemental Data include detailed experimental procedures and an image of the *brk1* hypocotyl epidermal adhesion phenotype and are available with this article online at: <http://www.current-biology.com/cgi/content/full/16/9/895/DC1/>.

Acknowledgments

We would like to thank Kendra Meade for combing the microarray databases for WAVE and ARP2/3 gene expression data. Thanks go to Youran Fan for his help with statistical analyses, to Laurie Smith for the kind gift of maize *brk1* seeds, and to Guri Johal group for helping us grow the mutant. Debbie Sherman at the Purdue Life Sciences Microscopy Center helped acquire the SEM images. We also thank the Purdue Cytoskeleton Group for useful discussions. The *Arabidopsis* Biological Resource Center distributed numerous key reagents. Work in the lab of D.B.S. was supported by grants from the National Science Foundation-Integrated Biology and Neuroscience (IBN-0416546) and Department of Energy-Energy Biosciences Division (DE-FG02-02ER15357).

Received: January 23, 2006

Revised: March 6, 2006

Accepted: March 7, 2006

Published online: April 6, 2006

References

1. Kaksonen, M., Sun, Y., and Drubin, D.G. (2003). A pathway for association of receptors, adaptors, and actin during endocytic internalization. *Cell* 115, 475–487.
2. Eitzen, G., Wang, L., Thorngren, N., and Wickner, W. (2002). Remodeling of organelle-bound actin is required for yeast vacuole fusion. *J. Cell Biol.* 158, 669–679.
3. Mathur, J., Mathur, N., Kernebeck, B., and Hulskamp, M. (2003). Mutations in actin-related proteins 2 and 3 affect cell shape development in *Arabidopsis*. *Plant Cell* 15, 1632–1645.
4. Svitkina, T.M., and Borisy, G.G. (1999). Arp2/3 and actin depolymerizing factor/cofilin in dendritic organization and treadmilling of actin filament array in lamellipodia. *J. Cell Biol.* 145, 1009–1026.
5. Chen, J.L., Lacomis, L., Erdjument-Bromage, H., Tempst, P., and Stamnes, M. (2004). Cytosol derived proteins are sufficient for Arp2/3 recruitment and ARF/coatomer-dependent actin polymerization on Golgi membranes. *FEBS Lett.* 566, 281–285.
6. Yan, C., Martinez-Quiles, N., Eden, S., Shibata, T., Takeshima, F., Shinkura, R., Fujiwara, Y., Bronson, R., Snapper, S.B., Kirschner, M.W., et al. (2003). WAVE2 deficiency reveals distinct roles in embryogenesis and Rac-mediated actin-based motility. *EMBO J.* 22, 3602–3612.
7. Bogdan, S., and Klambt, C. (2003). Kette regulates actin dynamics and genetically interacts with Wave and Wasp. *Development* 130, 4427–4437.
8. Blagg, S.L., Stewart, M., Sambles, C., and Insall, R.H. (2003). PIR121 regulates pseudopod dynamics and SCAR activity in *Dictyostelium*. *Curr. Biol.* 13, 1480–1487.
9. Basu, D., Le, J., El-Assal, S.E., Huang, C., Zhang, C., Mallery, E.L., Koliantz, G., Staiger, C.J., and Szymanski, D.B. (2005). DISTORTED3/SCAR2 is a putative *Arabidopsis* WAVE complex subunit that activates the Arp2/3 complex and is required for epidermal morphogenesis. *Plant Cell* 17, 502–524.
10. Eden, S., Rohatgi, R., Podtelejnikov, A.V., Mann, M., and Kirschner, M.W. (2002). Mechanism of regulation of WAVE1-induced actin nucleation by Rac1 and Nck. *Nature* 418, 790–793.
11. Kunda, P., Craig, G., Dominguez, V., and Baum, B. (2003). Abi, Sra1, and Kette control the stability and localization of SCAR/WAVE to regulate the formation of actin-based protrusions. *Curr. Biol.* 13, 1867–1875.
12. Steffen, A., Rottner, K., Ehinger, J., Innocenti, M., Scita, G., Wehland, J., and Stradal, T.E.B. (2004). Sra-1 and Nap1 link Rac to actin assembly driving lamellipodia formation. *EMBO J.* 23, 749–759.
13. Innocenti, M., Zucconi, A., Disanza, A., Frittoli, E., Areces, L.B., Steffen, A., Stradal, T.E.B., Di Fiore, P.P., Carlier, M.-F., and Scita, G. (2004). Abi1 is essential for the formation and activation of a WAVE2 signaling complex mediating Rac-dependent actin remodeling. *Nat. Cell Biol.* 6, 319–327.
14. Szymanski, D.B. (2005). Breaking the WAVE complex: The point of *Arabidopsis* trichomes. *Curr. Opin. Plant Biol.* 8, 103–112.
15. Mathur, J., Spielhofer, P., Kost, B., and Chua, N. (1999). The actin cytoskeleton is required to elaborate and maintain spatial patterning during trichome cell morphogenesis in *Arabidopsis thaliana*. *Development* 126, 5559–5568.
16. Szymanski, D.B., Marks, M.D., and Wick, S.M. (1999). Organized F-actin is essential for normal trichome morphogenesis in *Arabidopsis*. *Plant Cell* 11, 2331–2347.
17. Deeks, M.J., Kaloriti, D., Davies, B., Malho, R., and Hussey, P.J. (2004). *Arabidopsis* NAP1 is essential for ARP2/3-dependent trichome morphogenesis. *Curr. Biol.* 14, 1410–1414.
18. Zhang, X., Dyachok, J., Krishnakumar, S., Smith, L.G., and Oppenheimer, D.G. (2005). IRREGULAR TRICHOME BRANCH1 in *Arabidopsis* encodes a plant homolog of the actin-related protein2/3 complex activator Scar/WAVE that regulates actin and microtubule organization. *Plant Cell* 17, 2314–2326.
19. Machesky, L.M., Mullins, R.D., Higgs, H.N., Kaiser, D.A., Blanchoin, L., May, R.C., Hall, M.E., and Pollard, T.D. (1999). Scar, a WASp-related protein, activates nucleation of actin filaments by the Arp 2/3 complex. *Proc. Natl. Acad. Sci. USA* 96, 3739–3744.

20. Suetsugu, S., Miki, H., and Takenawa, T. (1999). Identification of two human WAVE/SCAR homologues as general actin regulatory molecules which associate with the Arp2/3 complex. *Biochem. Biophys. Res. Commun.* **260**, 296–302.
21. Stradal, T.E., and Scita, G. (2006). Protein complexes regulating Arp2/3-mediated actin assembly. *Curr. Opin. Cell Biol.* **18**, 1–7.
22. McCallum, C.M., Comai, L., Greene, E.A., and Henikoff, S. (2000). Targeting induced local lesions in genomes (TILLING) for plant functional genomics. *Plant Physiol.* **123**, 439–442.
23. Frank, M.J., and Smith, L.G. (2002). A small, novel protein highly conserved in plants and animals promotes the polarized growth and division of maize leaf epidermal cells. *Curr. Biol.* **12**, 849–853.
24. Schmid, M., Davison, T.S., Henz, S.R., Pape, U.J., Demar, M., Vingron, M., Scholkopf, B., Weigel, D., and Lohmann, J.U. (2005). A gene expression map of *Arabidopsis thaliana* development. *Nat. Genet.* **37**, 501–506.
25. Li, Y., Sorefan, K., Hemmann, G., and Bevan, M.W. (2004). *Arabidopsis* NAP and PIR regulate actin-based cell morphogenesis and multiple developmental processes. *Plant Physiol.* **136**, 3616–3627.
26. Le, J., El-Assal, S.E., Basu, D., Saad, M.E., and Szymanski, D.B. (2003). Requirements for *Arabidopsis* ATARP2 and ATARP3 during epidermal development. *Curr. Biol.* **13**, 1341–1347.
27. El-Assal, S.E., Le, J., Basu, D., Mallery, E.L., and Szymanski, D.B. (2004). *DISTORTED2* encodes an ARPC2 subunit of the putative *Arabidopsis* ARP2/3 complex. *Plant J.* **38**, 526–538.
28. El-Assal, S.E., Le, J., Basu, D., Mallery, E.L., and Szymanski, D.B. (2004). *Arabidopsis* GNARLED encodes a NAP125 homologue that positively regulates ARP2/3. *Curr. Biol.* **14**, 1405–1409.
29. Basu, D., El-Assal, S.E., Le, J., Mallery, E.L., and Szymanski, D.B. (2004). Interchangeable functions of *Arabidopsis* PIROGI and the human WAVE complex subunit SRA-1 during leaf epidermal morphogenesis. *Development* **131**, 4345–4355.
30. Li, S., Blanchoin, L., Yang, Z., and Lord, E.M. (2003). The putative *Arabidopsis* Arp2/3 complex controls leaf cell morphogenesis. *Plant Physiol.* **132**, 2034–2044.
31. Brembu, T., Winge, P., Seem, M., and Bones, A.M. (2004). NAPP and PIRP encode subunits of a putative Wave regulatory proteins complex involved in plant cell morphogenesis. *Plant Cell* **16**, 2335–2349.
32. Saedler, R., Zimmermann, I., Mutondo, M., and Hulskamp, M. (2004). The *Arabidopsis* KLUNKER gene controls cell shape changes and encodes the AtSRA1 homolog. *Plant Mol. Biol.* **56**, 775–782.
33. Russ, J.C. (2002). *The Image Processing Handbook*, Fourth Edition (Boca Raton: CRC Press).
34. Kieber, J., Rothenberg, M., Roman, G., Feldmann, K., and Ecker, J. (1993). *CTR1*, a negative regulator of the ethylene response pathway in *Arabidopsis*, encodes a member of the Raf family of protein kinases. *Cell* **72**, 427–441.
35. Frank, M.J., Cartwright, H.N., and Smith, L.G. (2003). Three Brick genes have distinct functions in a common pathway promoting polarized cell division and cell morphogenesis in the maize leaf epidermis. *Development* **130**, 753–762.
36. Panteris, E., Apostolakis, P., and Galatis, B. (1994). Sinuous ordinary epidermal cells: Behind several patterns of waviness, a common morphogenetic mechanism. *New Phytol.* **127**, 771–780.
37. Qiu, J.L., Jilk, R., Marks, M.D., and Szymanski, D.B. (2002). The *Arabidopsis* SPIKE1 gene is required for normal cell shape control and tissue development. *Plant Cell* **14**, 101–118.
38. Fu, Y., Gu, Y., Zheng, Z., Wasteneys, G.O., and Yang, Z. (2005). *Arabidopsis* interdigitating cell growth requires two antagonistic pathways with opposing action on cell morphogenesis. *Cell* **11**, 687–700.
39. Gautreau, A., Ho, H.H., Steen, H., Gygi, S.P., and Kirschner, M.W. (2004). Purification and architecture of the ubiquitous Wave complex. *Proc. Natl. Acad. Sci. USA* **101**, 4379–4383.
40. Frank, M., Egile, C., Dyachok, J., Djakovic, S., Nolasco, M., Li, R., and Smith, L.G. (2004). Activation of Arp2/3 complex-dependent actin polymerization by plant proteins distantly related to Scar/WAVE. *Proc. Natl. Acad. Sci. USA* **101**, 16379–16384.
41. Kobayashi, K., Kuroda, S., Fukata, M., Nakamura, T., Nagase, T., Nomura, N., Matsuura, Y., Yoshida-Kubomura, N., Iwamatsu, A., and Kaibuchi, K. (1998). p140Sra-1 (specifically Rac1-associated protein) is a novel specific target for Rac1 small GTPase. *J. Biol. Chem.* **273**, 291–295.
42. Schenck, A., Qurashi, A., Carrera, P., Bardoni, B., Diebold, C., Schejter, E., Mandel, J.L., and Giangrande, A. (2004). WAVE/SCAR, a multifunctional complex coordinating different aspects of neuronal connectivity. *Dev. Biol.* **274**, 260–270.